Numerical Study of Axisymmetric Dielectric Resonators

Shouyuan Shi, Liuqing Yang, and Dennis W. Prather

***Abstract*—In this paper, we present an effective approach to study the behavior of axisymmetric dielectric resonators. This approach is based on the finite-difference time-domain method and two accompanying techniques in order to increase the accuracy and decrease the computational cost. These two techniques are the fast-Fourier-transform approach and the Padé method. This method is used to obtain the resonant frequencies and quality factors for several resonators. Comparisons are made to show the utility of the method.**

***Index Terms*—Dielectric resonators, FDTD method, Q-factors.**

I. Introduction

RECENTLY, dielectric resonators based on axisymmetric structures have been widely studied. In these studies, the calculation of resonant modes is very important. Unfortunately, analytic solutions are available only for very simple geometries, such as homogeneous and cavities bounded by perfectly conducting surfaces. However, in most practical applications, the resonators usually contain complex structures, such as inhomogeneities and complicated boundary conditions. As a result, the resonant frequencies and Q-factors—which are crucial parameters in the design of resonators—are very difficult to analyze. In these cases, the cavities must be analyzed using numerical techniques.

One such technique is the finite-difference time-domain (FDTD) technique, which has been employed in the past for the analysis of various types of cavities and open dielectric resonators [1]–[3]. The advantage of the FDTD technique over alternate frequency-domain methods, such as the method of moments (MoM) and finite-element method (FEM), is that resonant frequencies of all modes can be calculated in a single simulation by using the time-domain nature of the method rather than individually sweeping the frequency to capture each mode.

To obtain the resonant frequencies and the quality factors (Q-factors) using the FDTD, one must transform the time-dependent response of the FDTD simulation to the frequency domain, say, by using the fast Fourier transform (FFT). After performing the FFT on the FDTD output data, we can derive the resonant frequencies from the local maxima of the response. The Q-factors can then be computed from the following expression:

$$Q = \frac{f_0}{\Delta f} \tag{1}$$

where Δf is the 3-dB bandwidth and f_0 is the resonant frequency.

To calculate the resonant frequencies and Q-factors with high accuracy and resolution using the FFT method requires a significant number of time samples, which, in turn, requires a long computational time. To overcome this limitation, alternate procedures have been proposed [1]. Two commonly employed techniques are the Prony's method and generalized-pencil-of-function technique, both of which eliminate the need for an FFT by expanding the time-dependent response in a sum of exponentials. Although both of these methods have advantages over the FFT technique in terms of the reduction in the computational time, the accuracy of these methods is very sensitive to the sampling conditions.

In this paper an alternative approach that uses the Padé approximation in conjunction with the FFT technique to overcome the above limitations is employed. As a result, our model is very effective in determining the resonant frequencies and the Q-factors in a relatively small time window, which thereby reduces computational cost. In addition, in most FDTD simulations, the computational area is 5–10 times larger than the area of the cavity, or resonator, in order to reduce the effects of reflection from the sidewalls. However, such a large FDTD computational region significantly increase both the computational time and memory requirements. Therefore, in our approach, the perfectly matched layer (PML) [4], [5] is employed, which allows the absorbing boundary to be placed much closer to the resonator. As a result, in comparison to previous techniques [1], [2], our computational time is considerably less.

In Section II, we discuss our method and its use for the analysis of an axisymmetric perfectly electric conductor (PEC) bounded cavity and an open dielectric resonator. Several numerical results and comparisons are presented in Section III.

II. Theory

A. Axially Symmetric FDTD Method

For an axially symmetric geometry, or so-called body of revolution (BOR), as shown in Fig. 1, one can use a simplified two-and-one-half dimensional (2.5-D) FDTD algorithm [6] instead of a full three-dimensional (3-D) technique, as described in [7].

To show this, we begin with the assumption that the angular variation of the electromagnetic fields has either a $\sin k\phi$ or $\cos k\phi$ dependence. For axisymmetric structures, the dependence of field components on ϕ can be represented into

Manuscript received August 19, 2000.

The authors are with the Department of Electrical and Computer Engineering, University of Delaware, Newark, DE 19716 USA (e-mail: dprather@ee.udel.edu).

Publisher Item Identifier S 0018-9480(01)07587-1.

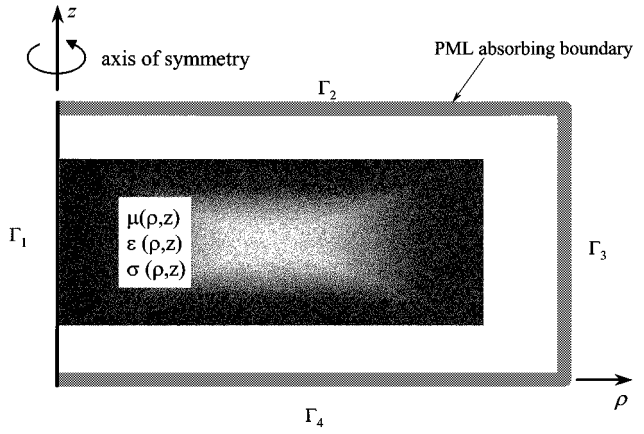

Fig. 1. Geometry of axisymmetric resonators.

a Fourier series expansion. For example, the electric field $E_\rho(\rho,\phi,z,t)$ is given by

$$E_\rho(\rho,\phi,z,t) = E_{\rho,0}(\rho,z,t) + \sum_{k=1}^{\infty} E_{\rho,k}(\rho,z,t)\cos(k\phi) + \sum_{k=1}^{\infty} E'_{\rho,k}(\rho,z,t)\sin(k\phi) \quad (2)$$

with the Fourier coefficients

$$\begin{aligned} E_{\rho,0}(\rho,z,t) &= \frac{1}{2\pi}\int_0^{2\pi} E_\rho(\rho,\phi,z,t)\,d\phi \\ E_{\rho,k}(\rho,z,t) &= \frac{1}{\pi}\int_0^{2\pi} E_\rho(\rho,\phi,z,t)\cos(k\phi)\,d\phi \\ E'_{\rho,k}(\rho,z,t) &= \frac{1}{\pi}\int_0^{2\pi} E_\rho(\rho,\phi,z,t)\sin(k\phi)\,d\phi. \end{aligned} \quad (3)$$

In this manner, there will be two independent sets of difference equations. The field components in one set are rotated 90° with respect to those in another set. Considering that results obtained from each of the two sets will show the same resonance property, we selected to use only one of them, in which the cosinusoidal terms of H_ϕ, E_ρ, and E_z and the sinusoidal terms of E_ϕ, H_ρ, and H_z are used. Since the Fourier modes in the series expansion are mutually orthogonal, one can solve for the electromagnetic fields for each mode independently. Furthermore, for each different mode k, the differentiation with respect to ϕ reduces the full 3-D problem to an equivalent 2.5-D one. Therefore, the Maxwell's curl equations can be expressed as

$$\begin{aligned} \mu\frac{\partial H_{\rho,k}}{\partial t} &= \frac{k}{\rho}E_{z,k} + \frac{\partial E_{\phi,k}}{\partial z} \\ \mu\frac{\partial H_{\phi,k}}{\partial t} &= -\frac{\partial E_{\rho,k}}{\partial z} + \frac{\partial E_{z,k}}{\partial \rho} \\ \mu\frac{\partial H_{z,k}}{\partial t} &= -\frac{1}{\rho}\frac{\partial(\rho E_{\phi,k})}{\partial \rho} - \frac{k}{\rho}E_{\rho,k} \end{aligned} \quad (4)$$

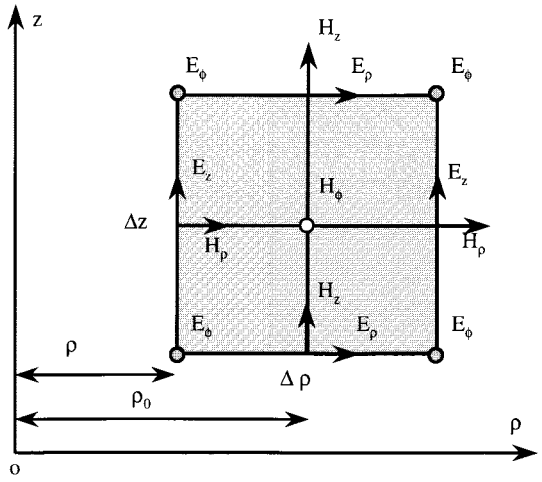

(a)

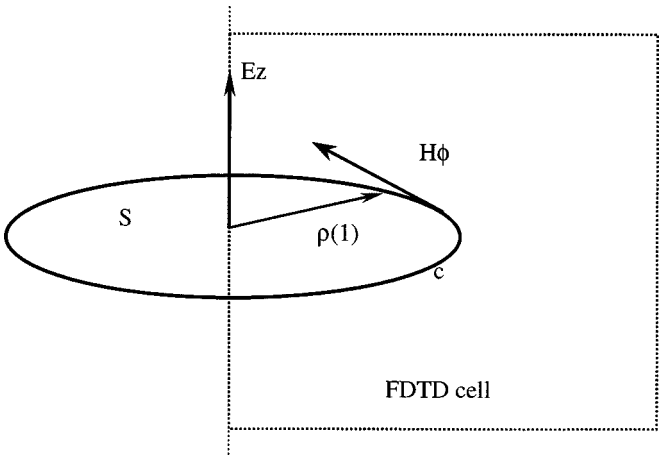

(b)

Fig. 2. FDTD mesh for an axially symmetric computational region. (a) Off-axis mesh. (b) On-axis mesh.

and

$$\begin{aligned} \varepsilon\frac{\partial E_{\rho,k}}{\partial t} + \sigma E_{\rho,k} &= \frac{k}{\rho}H_{z,k} - \frac{\partial H_{\phi,k}}{\partial z} \\ \varepsilon\frac{\partial E_{\phi,k}}{\partial t} + \sigma E_{\phi,k} &= \frac{\partial H_{\rho,k}}{\partial z} - \frac{\partial H_{z,k}}{\partial \rho} \\ \varepsilon\frac{\partial E_{z,k}}{\partial t} + \sigma E_{z,k} &= \frac{1}{\rho}\frac{\partial(\rho H_{\phi,k})}{\partial \rho} - \frac{k}{\rho}H_{\rho,k} \end{aligned} \quad (5)$$

where σ is conductivity and the electromagnetic fields are expressed in cylindrical coordinates.

Next, the FDTD method can be used to simulate the scattering of an axially symmetric geometry. To do this, the whole computational region is divided into several parts, as shown in Fig. 1.

If we now assume that the electromagnetic-field components are assigned as illustrated in Fig. 2, we can apply the central difference method to (4) and (5), which can be rewritten as

$$\begin{aligned} &H_\rho^n(I,J) \\ &\quad = H_\rho^{n-1}(I,J) + \frac{k\Delta t}{\mu\rho(I)}E_z^{n-1/2}(I,J) \\ &\qquad + \frac{\Delta t}{\mu\Delta z}\left[E_\phi^{n-1/2}(I,J+1) - E_\phi^{n-1/2}(I,J)\right] \end{aligned}$$

$$
\begin{aligned}
&H_\phi^n(I,J) \\
&\quad = H_\phi^{n-1}(I,J) - \frac{\Delta t}{\mu \Delta z} \\
&\qquad \times \left[E_\rho^{n-1/2}(I,J+1) - E_\rho^{n-1/2}(I,J)\right] \\
&\qquad + \frac{\Delta t}{\mu \Delta \rho}\left[E_z^{n-1/2}(I+1,J) - E_z^{n-1/2}(I,J)\right] \\
&H_z^n(I,J) \\
&\quad = H_z^{n-1}(I,J) - \frac{k\Delta t}{\mu\rho\left(I+\frac{1}{2}\right)} E_\rho^{n-1/2}(I,J) \\
&\qquad - \frac{\Delta t}{\mu \Delta \rho \rho\left(I+\frac{1}{2}\right)} \\
&\qquad \times \left[\rho(I+1) E_\phi^{n-1/2}(I+1,J) - \rho(I) E_\phi^{n-1/2}(I,J)\right] \\
&E_\rho^{n+1/2}(I,J) \\
&\quad = \frac{2\varepsilon - \sigma\Delta t}{2\varepsilon + \sigma \Delta t} E_\rho^{n-1/2}(I,J) \\
&\qquad + \frac{2k\Delta t}{\rho\left(I+\frac{1}{2}\right)(2\varepsilon + \sigma\Delta t)} H_z^n(I,J) \\
&\qquad - \frac{\frac{2\Delta t}{\Delta z}}{2\varepsilon + \sigma \Delta t}\left[H_\phi^n(I,J) - H_\phi^n(I,J-1)\right]
\end{aligned} \tag{6}
$$

$$
\begin{aligned}
&E_\phi^{n+1/2}(I,J) \\
&\quad = \frac{2\varepsilon - \sigma\Delta t}{2\varepsilon + \sigma \Delta t} E_\phi^{n-1/2}(I,J) + \frac{\frac{2\Delta t}{\Delta z}}{2\varepsilon + \sigma \Delta t} \\
&\qquad \times \left[H_\rho^n(I,J) - H_\rho^n(I,J-1)\right] \\
&\qquad - \frac{\frac{2\Delta t}{\Delta \rho}}{2\varepsilon + \sigma \Delta t}\left[H_z^n(I,J) - H_z^n(I-1,J)\right] \\
&E_z^{n+1/2}(I,J) \\
&\quad = \frac{2\varepsilon - \sigma\Delta t}{2\varepsilon + \sigma \Delta t} E_z^{n-1/2}(I,J) \\
&\qquad - \frac{2k\Delta t}{\rho(I)(2\varepsilon + \sigma\Delta t)} H_\rho^n(I,J) \\
&\qquad + \frac{\frac{2\Delta t}{\Delta \rho}}{\rho(I)(2\varepsilon + \sigma\Delta t)}\left[\rho\left(I+\frac{1}{2}\right) H_\phi^n(I,J)\right. \\
&\qquad\qquad \left. - \rho\left(I-\frac{1}{2}\right) H_\phi^n(I-1,J)\right]
\end{aligned} \tag{7}
$$

where $\rho(x) = x \cdot \Delta\rho$ ($x = I-(1/2), I, I+(1/2)$ or $I+1$), $\Delta\rho$, and Δz are discretization length in the ρ- and z-directions, respectively, and Δt is time step that satisfies the dispersion condition [7]

$$
c\Delta t \le \frac{\Delta}{s}, \qquad \text{where } s = 2\,(k=0) \text{ and } s = k+1 \ (k \geqslant 1). \tag{8}
$$

From Fig. 2, we see that only the E_z, E_ϕ, and H_ρ components lie on the axis. However, only the E_z component along the axis needs to be computed because the on-axis components of E_ϕ and H_ρ are not necessary to update the FDTD fields. Furthermore, E_z only needs to be computed for the $k=0$ mode since this component equals zero for all $k > 0$ modes. This follows from the fact that any constant-ρ path integral resulting from Faraday's Law, about $\rho = 0$, integrates to zero for $k > 0$. Thus, the equation for computation of $E_{z,0}$ is given as

$$
\varepsilon \frac{\partial E_{z,0}}{\partial t} + \sigma E_{z,0} = \frac{4}{\rho(1)} H_{\phi,0}. \tag{9}
$$

As shown in Fig. 1, the computational region is surrounded by Γ_1, Γ_2, Γ_3, and Γ_4, on which the appropriate boundary conditions are needed to truncate the region and to reduce unwanted reflections. No absorbing boundary condition (ABC) is needed for the Γ_1 boundary because the wave toward the axial center is a standing wave rather than a propagating wave. To simulate free space outside the resonator, the perfectly matched layer (PML) is introduced on boundaries Γ_2, Γ_3, and Γ_4. Previously presented approaches did not use PMLs, Γ_2, Γ_3, and Γ_4, and, therefore, placed them at a sufficiently large distances away (generally two or three times the size of the disk) from the disk to avoid inaccuracies or instabilities caused by reflection back reflections [1], [2]. In our approach, since we use the PML, the boundaries Γ_2, Γ_3, and Γ_4 can be put as close as ten or 15 FDTD cells to the resonator without introducing any inaccuracy or instability. Therefore, the FDTD computational region is truncated to one that is considerably smaller, which significantly reduces memory requirements and computational time. In the case of an open dielectric resonator, no condition needs to be applied on the surface of the resonator, and in the case of a cavity bounded by perfectly conducting boundaries, we need only to set the tangential fields to zero on these boundaries.

To apply the PML, we employed the complex coordinate stretching method [4], [5] to derive the anisotropic PML ABC, which was given by

$$
\begin{aligned}
\nabla \times \mathbf{E} &= -j\omega\mu[\Lambda]\mathbf{H} \\
\nabla \times \mathbf{H} &= j\omega\varepsilon[\Lambda]\mathbf{E}
\end{aligned} \tag{10}
$$

where

$$
[\Lambda] = \hat{\rho}\hat{\rho}\frac{s_\phi s_z}{s_\rho} + \hat{\phi}\hat{\phi}\frac{s_\rho s_z}{s_\phi} + \hat{z}\hat{z}\frac{s_\rho s_\phi}{s_z} \tag{11}
$$

and

$$
\begin{aligned}
s_\rho &= 1 - j\frac{\sigma_\rho}{\omega\varepsilon_0} \\
s_\phi &= \frac{1}{\rho}\int_0^\rho \left(1 - j\frac{\sigma_\rho}{\omega\varepsilon_0}\right) d\rho' = 1 - j\frac{\gamma_\rho}{\omega\varepsilon_0} \\
s_z &= 1 - j\frac{\sigma_z}{\omega\varepsilon_0}.
\end{aligned} \tag{12}
$$

To do this, we first transform the modified Maxwell equations to the time domain and then use the central-difference method to discretize the equations and apply the FDTD [6].

In order to obtain resonant frequencies of different modes in *one* simulation, several Gaussian pulses localized inside the resonator are used. The reason we used more than one excitation

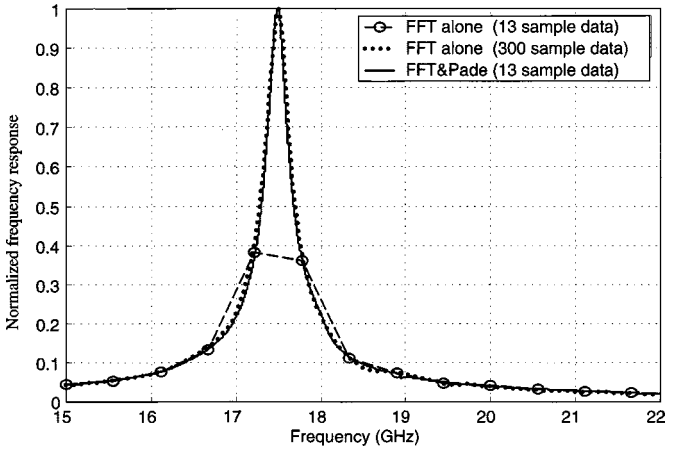

Fig. 3. Normalized frequency response of a dielectric disk: radius $= 8$ mm thickness $= 1.8$ mm, permittivity $= 12.25$. This is the HE_{41} mode.

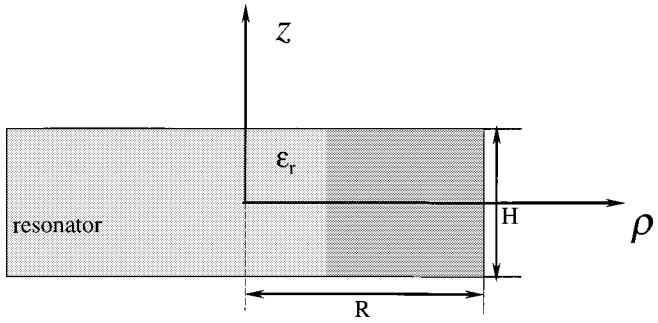

Fig. 4. Cross section of a dielectric resonator with radius $R = 5.25$ mm, thickness $H = 4.62$ mm, and relative permittivity $\varepsilon_r = 38$.

is that a mode can be missed if the single excitation is placed at the null field points of the mode. In our method, such a miss is avoided by placing excitations at different locations. At any other points inside the resonator, the fields can be recorded for each iteration for subsequent use in determining the resonant frequencies and Q-factors. By using the FFT method, the responses can be transformed to the frequency domain to obtain the frequency response.

B. Extrapolation of Resonant Frequencies and Q-Factors

As discussed above, the FFT approach is limited due to the extremely long execution time needed to obtain accurate resonant frequencies and Q-factors. In this section, we will present an effective method that combines the FFT technique with the Padé approximation [3].

This approach is based on the Padé approximation, which is an effective mathematical technique used to interpolate the resonant frequencies and Q-factors. To overcome the limitation of the FFT method, we employ the Padé approximation in conjunction with the FFT scheme in a two-step process. First, we apply the FFT on the FDTD results to obtain a coarse response. The response is then further processed using the Padé approximation to obtain the accurate resonant frequencies and Q-factors.

The coarse response obtained by applying the FFT can be represented as a sum of pole series

$$P(\omega) = P_p(\omega) + P_{np}(\omega) \tag{13}$$

TABLE I
RESONANT FREQUENCIES AS DETERMINED USING THE ANALYTICAL METHOD, THE FFT APPROACH, AND THE FFT TECHNIQUE IN COMBINATION WITH THE PADÉ APPROXIMATION. THE PERCENTAGE ERRORS ARE ALSO LISTED

Modes	Analytical Result	FFT		FFT&Pade	
	(GHz)	*(GHz)*	Error(%)	*(GHz)*	Error(%)
HEM_{121}	8.3177	8.3200	0.0277	8.3172	0.0060
HEM_{211}	7.4995	7.4707	0.3840	7.4979	0.0213
HEM_{221}	9.7139	9.6680	0.4725	9.6995	0.1482
HEM_{212}	11.8310	11.7554	0.6390	11.8217	0.0786
HEM_{311}	9.0250	8.9356	0.9906	8.9922	0.3634
HEM_{312}	12.8107	12.7442	0.5191	12.7618	0.3817
HEM_{331}	13.3215	13.1836	1.0352	13.2316	0.6478

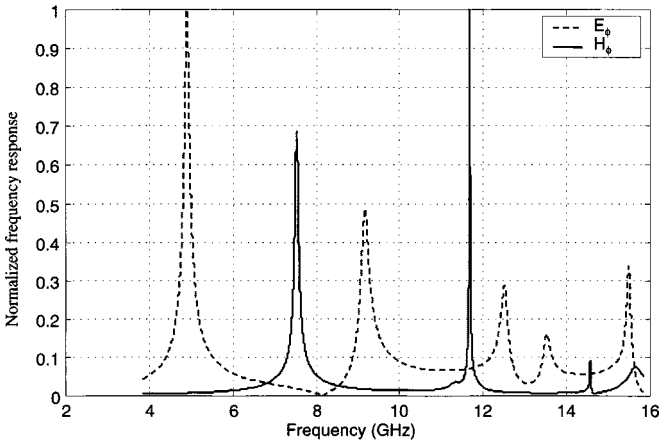

Fig. 5. Frequency-domain response after the Padé approximation.

TABLE II
Q-FACTORS OBTAINED USING THE FFT APPROACH AND THE FFT TECHNIQUE IN COMBINATION WITH THE PADÉ APPROXIMATION IN COMPARISON TO EXPERIMENTAL VALUES

Modes	Frequency	Q-factor		
	(GHz)	FFT (262,144 iterations)	FFT&Pade (3,000 iterations)	Experimental Value
$TE_{01\delta}$	4.8713	47.0000	50.1276	51
$HEM_{11\delta}$	6.3228	62.0000	65.3213	/
$TM_{01\delta}$	7.5083	86.0000	90.7005	86
$TE_{02\delta}$	9.1199	47.4286	49.0409	/

where $P(\omega)$ is a complex vector-valued function of ω representing one of the six electromagnetic components. The first term on the right-hand side of (13) contains all of the poles of $P(\omega)$ and the second term represents the remainder. The Padé approximation constitutes expressing $P_p(\omega)$ in a rational function as

$$P(\omega) = \frac{Q_N(\omega)}{D_M(\omega)} \tag{14}$$

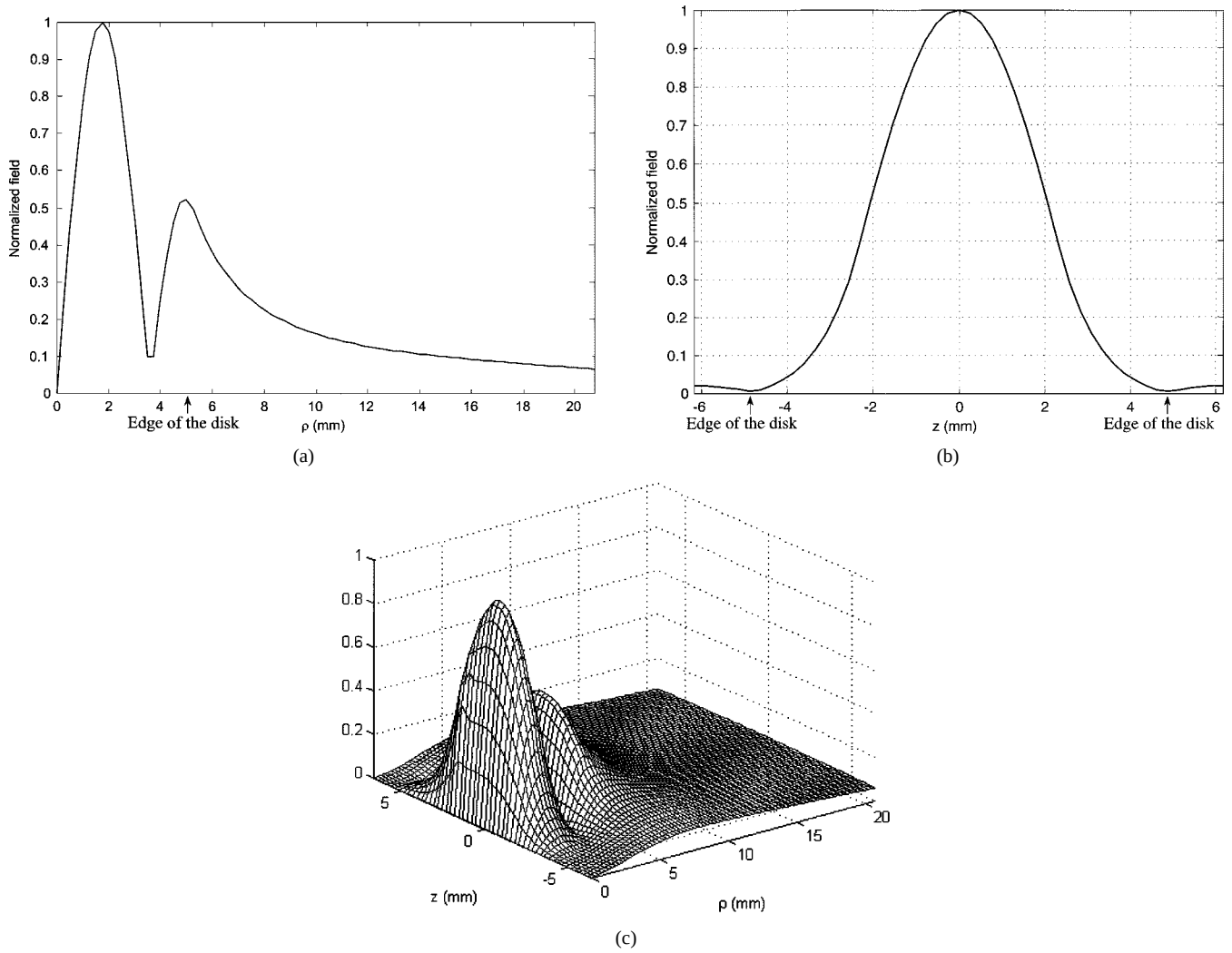

Fig. 6. (a) Radial distribution ($z = 0$ mm), (b) axial distribution ($\rho = 1.75$ mm), and (c) spatial distribution of the E_ϕ-field component for mode $\mathrm{TE}_{02\delta}$. The resonant frequency for this mode is 9.1199 GHz.

where the numerator and denominator polynomials $Q_N(\omega)$ and $D_M(\omega)$ are given by

$$Q_N(\omega) = \sum_{i=0}^{N} \alpha_i \omega^i$$

$$D_M(\omega) = \sum_{i=0}^{M} \beta_i \omega^i. \tag{15}$$

Now, $\{\alpha_i\}$ and $\{\beta_i\}$ are coefficients that need to be solved for. Let $P(\omega_j)$ denote the value of the frequency-domain response obtained from the FFT, which are going to be used as sample data at frequency ω_j. By setting $\beta_0 = 1$, (14) can be rewritten as

$$P(\omega_j)\sum_{i=1}^{M} \beta_i \omega^i - \sum_{i=0}^{N} \alpha_i \omega^i = -P(\omega_j), \qquad j=0,\ldots,s-1 \tag{16}$$

where s is the number of sample data, and there are $N+M+1$ unknowns. When the number of sampled data obtained from the FFT equals the number of unknowns, it is very easy to obtain the final answer. However, in most cases, the sampled data obtained from the FFT are different from the number of unknowns. Thus, the set of equations are thereby either overdetermined or underdetermined. Therefore, we apply the least square method to solve the equation under this situation. Once the coefficients of polynomials are determined, it is easy to interpolate the sampled data to obtain the desired resolution. In Fig. 3, the frequency responses obtained from the FFT alone and the FFT in conjunction with the Padé approximation are plotted. One can see that, to achieve the same accuracy, far less sampled data is needed by using the FFT and Padé approximation together rather than using the FFT alone. That means much less computational time is needed.

III. Numerical Results

To test the algorithm, we first studied a parallel-plate cylindrical dielectric resonator. A dielectric resonator of radius $R = 5.25$ mm, height of $H = 4.62$ mm, and relative permittivity $\varepsilon_r = 38$ has been considered and placed between two undefined metallic planes. Fig. 4 shows the cross section of the resonator. The origin of the ρ, z coordinate system is placed at the center of the disk. The reason we chose this cavity is because analytical

results exist and the resonant frequencies for different modes can be obtained [8] as follows:

$$\left(\frac{J'_m(u)}{u\cdot J_m(u)}+\frac{K'_m(w)}{w\cdot K_m(w)}\right)\cdot\left(\frac{J'_m(u)}{u\cdot J_m(u)}+\frac{n_2^2}{n_1^2}\cdot\frac{K'_m(w)}{w\cdot K_m(w)}\right)=\left(\frac{m\beta}{n_1k}\right)^2\cdot\left(\frac{v}{uw}\right)^4 \tag{17}$$

where $u = R\sqrt{k^2n_1^2-\beta^2}$, $w = R\sqrt{\beta^2-k^2n_2^2}$, $v = \sqrt{u^2+w^2}$, and $k = 2\pi f\sqrt{\mu_0\varepsilon_0}$. The propagation constant $\beta = p\pi/H$ conforms to the condition of stationary wave between the two metallic planes.

Table I presents the resonant frequencies as determined using the analytical method, FFT approach, and FFT technique in combination with the Padé approximation. For the Padé method, 2048, 4096, and 8192 time steps were used for the modes of 0, 1, and 2 in the azimuthal direction, respectively. For the FFT method alone, 32 768 time steps were used. As a result, the computational time was reduced by as much as a factor of 16. The comparison of resolution of the two methods is also given. The average percent error is 0.2392 for the Padé method, in comparison to 0.5811 for the FFT method alone.

The frequency response of mode 0 after the Padé approximation is shown in Fig. 5. Clearly, the Padé method shows a significant advantage, and the much higher resolution in far fewer time steps is very encouraging.

To test the validity (and in particular, the validity in estimating the Q-factors) of the method in open systems, we also applied our method to the study of an open dielectric resonator having a radius R, height H, and relative permittivity ε_r equal to the previous case.

To obtain reasonable (converged) results for the Q-factors when using the FFT alone, a time-stepping window extending over about 2^{17} (131 072) iterations was needed. However, using Padé method, only 3000 iterations were required. That represents a reduction in computational time of nearly 98%. The Q-factors obtained using the two methods and measured values [9] are listed in Table II.

The near-field distribution of the dominant field component E_ϕ for mode $\mathrm{TE}_{02\delta}$ is shown in Fig. 6. We can see that the field is strongly confined inside the cavity and decays outside the cavity.

IV. Conclusions

In this paper, we have employed the FDTD method with an alternative extrapolation method to analyze the dielectric resonator with parallel perfectly conducting plates and an open dielectric resonator. By comparison, the combination of the Padé method and FFT technique shows great advantage in reducing the computational time while producing an accurate solution. In addition, the application of a PML as an absorbing boundary enables the computational region to be kept small, thereby further reducing the computational cost. Also, the algorithm we proposed is not sensitive to input parameters, such as number of modes and sample data points, as are other methods that employ Prony's method.

References

[1] B. J. Li and P. L. Liu, "Numerical analysis of the whispering gallery modes by the finite-difference time-domain method," *IEEE J. Quantum Electron.*, vol. 32, pp. 1583–1587, Sept. 1996.

[2] A. Navarro and M. J. Nunez, "FDTD method coupled with FFT: A generalization to open cylindrical devices," *IEEE Trans. Microwave Theory Tech.*, vol. 42, pp. 870–874, May 1994.

[3] S. Dey and R. Mittra, "Efficient computation of resonant frequencies and quality factors of cavities via a combination of the finite-difference time-domain technique and the Padé approximation," *IEEE Microwave Guided Wave Lett.*, vol. 8, pp. 415–417, Dec. 1998.

[4] W. C. Chew and W. H. Weedon, "A 3D perfectly matched medium from modified Maxwell's equations with stretched coordinates," *Microwave Opt. Tech. Lett.*, vol. 7, pp. 599–604, 1994.

[5] F. L. Teixeira and W. C. Chew, "Systematic derivation of anisotropic PML absorbing media in cylindrical and spherical coordinates," *IEEE Microwave Guided Wave Lett.*, vol. 7, pp. 371–373, Nov. 1997.

[6] D. W. Prather and S. Shi, "Formulation and application of the finite-difference time-domain method for the analysis of axially-symmetric DOE's," *J. Opt. Soc. Amer. A, Opt. Image Sci.*, vol. 16, pp. 1131–1142, 1999.

[7] A. Taflove, *Computational Electromagnetics: The Finite-Difference Time Domain Method*. Norwood, MA: Artech, 1995.

[8] M. J. Adams, *An Introduction to Optical Waveguides*. New York: Wiley, 1981.

[9] D. Kajfez and P. Guillon, *Dielectric Resonators*. Norwood, MA: Artech, 1986.

Shouyuan Shi was born in Ninghai, Zhejiang, China, on February 8, 1969. He received the B.S., M.S., and Ph.D. degrees from Xidian University, Xidian, China, in 1991, 1994 and 1997 respectively, all in electrical engineering.

Since 1997 he has been a Post-Doctorate in the Department of Electrical Engineering, University of Delaware, Newark. His research interests include electromagnetic numerical modeling, electromagnetic imaging, antenna design, and analysis and synthesis of mesoscopic active and passive diffractive optical devices.

Liuqing Yang received the B.S.E.E. degree from the Huazhong University of Science and Technology, Huazhong, China, in 1990, and is currently working toward the Ph.D degree in electrical and computer engineering at the University of Delaware, Newark.

She is currently a Graduate Research Assistant in the Department of Electrical and Computer Engineering, University of Delaware. Her research interests include diffractive optical elements, microdisk lasers, and photonic bandgap (PBG) materials and their applications.

Dennis W. Prather is currently an Associate Professor in the Department of Electrical and Computer Engineering, University of Delaware, Newark.

He is currently performing research in the development of efficient electromagnetic models for both the analysis and synthesis of mesoscopic optical elements. He is also active in their fabrication, replication, and integration into hybrid opto-electronic systems.

Prof. Prather was the recipient of the 1999 National Science Foundation and Office of Naval Research Young Investigator Awards.